

7 Calibration Systems

A rigorous calibration strategy is a prerequisite for the unambiguous direct detection of hypothetical dark matter interactions in the LZ detector. The basic questions about any event are: (1) how did the particle interact, and (2) how much energy did it deposit? But before these questions can be answered, the (x,y,z,t) response of the LZ TPC must be understood.

The LZ calibration strategy is designed to accurately answer these questions, achieve the LZ science goals, and be ready to address the widest possible range of predicted dark-matter signatures. Basic requirements (referred to in this chapter as R-17nnnn for the different requirements) have been defined. The process for capturing requirements is described in Chapter 12. The principal calibration techniques planned for LZ have been used successfully in previous experiments, especially LUX and Zeplin. A summary of all sources to be used in LZ is included in Table 7.0.1.

Table 7.0.1: Baseline calibration sources for LZ.

Isotope	What	Purpose	Deployment	Custom?
Tritium	beta, $Q = 18.6$ keV	ER band	Internal	N
^{83m}Kr	beta/gamma, 32.1 keV and 9.4 keV	TPC (x, y, z)	Internal	Y
^{131m}Xe	164 keV γ	TPC (x, y, z) , Xe skin	Internal	Y
^{220}Rn	various α 's	xenon skin	Internal	N
AmLi	(α, n)	NR band	CSD	Y
^{252}Cf	spontaneous fission	NR efficiency	CSD	N
^{57}Co	122 keV γ	Xe skin threshold	CSD	N
^{228}Th	2.615 MeV γ , various others	OD energy scale	CSD	N
^{22}Na	back-to-back 511 keV γ 's	TPC and OD sync	CSD	N
$^{88}\text{Y Be}$	152 keV neutron	low-energy NR response	External	N
$^{205}\text{Bi Be}$	88.5 keV neutron	low-energy NR response	External	Y
$^{206}\text{Bi Be}$	47 keV neutron	low-energy NR response	External	Y
DD	2,450 keV neutron	NR light and charge yields	External	N
DD	272 keV neutron	NR light and charge yields	External	Y

As described in Chapter 1.3.1, signals in LZ consist of scintillation photons (S1) and ionized electrons, read-out as proportional scintillation (S2). Variation in the (x,y,z) response of S1 and the (x,y) of S2 arise, for example, from detector geometry, light collection and other factors. Variation in the (z,t) response of S2 could arise from changes in xenon purity, via attachment of ionized electrons by impurities. These calibrations will be addressed by mono-energetic internal radioisotope sources (Section 7.1).

Once these variations have been calibrated, it is possible to address the two questions posed in the first paragraph. The answer is contained in a plot like Figure 1.3.11 from Section 1.3.4, which shows the distri-

bution of background-like events (top) and expected signal-like events (bottom). These bands were obtained from in-situ calibration of the LUX detector. Similar techniques will be used for LZ, as described in detail in the following sections. In Figure 1.3.11, the overlaid curves of approximate event energy are obtained from a knowledge of the absolute photon and electron detection efficiency of the instrument. This in turn is obtained from mono-energetic photon interactions in the detector.

In addition to the broad spectrum nuclear recoil response, LZ will measure the absolute response of LXe to nuclear recoils. It is critical to make this calibration in-situ and LZ will be able to make more precise measurements than are presently available. This is due to its large target mass and extremely low background count rate. These measurements are discussed in Section 7.3 and Section 7.4.

7.1 Internal Radioisotope Sources

Liquid Xenon’s strong self-shielding ability, of great benefit to the dark matter search by largely eliminating external backgrounds from the central fiducial volume, conversely makes low-energy electron recoil calibrations of this central volume practically impossible using external radioisotope sources. Rather than rely on extremely long duration ($\gg 1$ d) exposures to high-rate high-energy (> 1 MeV) sources, gaseous radioisotopes will be mixed into the LXe itself. This ‘internal’ calibration source strategy has been well-demonstrated in LUX.

7.1.1 Metastable Krypton 83 (^{83m}Kr)

Metastable ^{83m}Kr is a low-energy (41 keV) monoenergetic source that is easy to produce and exhibits a conveniently short decay time (half-life of 1.8 h). The monoenergetic peak enables the production of high-resolution 3-D maps of S1 and S2 detector response, producing a calibration of spatially-varying detector efficiency effects. Electron drift efficiency, extraction efficiency, and S2 light production efficiency are each individually position-dependent, and can combine to produce a larger spatial variation in S2 response, one that can also be time-varying with changes in liquid purity. This motivates requirements R-170002 and R-170007, which necessitate a mono-energetic dispersed throughout the xenon. For all these reasons, regular (\sim weekly) 3-D detector response maps are essential to attaining the needs of the WIMP search.

It should be noted that ^{83m}Kr ’s decay occurs in two steps, separated by a short decay half-life ($\tau = 154$ ns). This timing variation from decay to decay produces a variation from event to event in the overall electron recombination probability, meaning that while ^{83m}Kr is quite useful as a monoenergetic peak source, its unusual recombination physics means it is not useful for mimicking typical electron recoil backgrounds.

^{83m}Kr production and handling for liquid noble detectors is now a mature process: a radon-pure charcoal is infused with a ^{83}Rb -containing aqueous solution, baked, and then placed in standard VCR plumbing (contained by particulate filters) to produce a ^{83m}Kr -generating source. To ‘inject’ ^{83m}Kr into the detector, a xenon carrier gas flows over the charcoal, carrying some ^{83m}Kr activity into the main xenon circulation path, with the dosed activity controllable by carrier gas flow rate and flow duration. As a noble gas, ^{83m}Kr has the practical advantage of first passing through the circulation path getter, for added protection against the incidental injection of impurities. ^{83}Rb has a conveniently long half-life of 86.2 days, meaning a single ^{83m}Kr source can sustain a usable activity for approximately one year.

7.1.2 Metastable Xenon 131 (^{131m}Xe)

Calibrations of the position reconstruction itself, essential to rejecting spatially-varying external backgrounds and to precisely defining a fiducial volume, are easiest if the calibration source activity is homogeneously

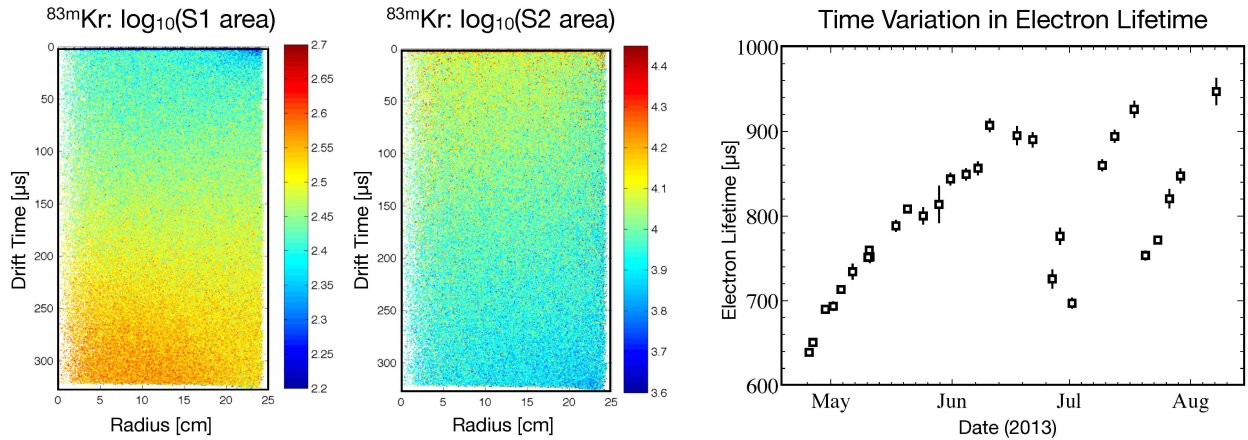


Figure 7.1.1: Several illustrations of $^{83\text{m}}\text{Kr}$ calibrations in LUX: (left) S1 area in the radius vs. drift time plane, (middle) S2 area in the same projection (on a particular date), and (right) a time-dependent measurement of electron lifetime in the drift region.

distributed throughout the active LXe. The liquid mixing timescale in LZ may not allow $^{83\text{m}}\text{Kr}$ to become fully homogeneous given its short decay timescale, and for this reason a $^{131\text{m}}\text{Xe}$ source is being developed as a long-lived alternative for the specific goal of achieving homogeneity (cf. requirements R-170002 and R-170007). Compared with $^{83\text{m}}\text{Kr}$, $^{131\text{m}}\text{Xe}$ decays at a higher energy (164 keV) and with a longer half-life (11.9 d). The higher energy may result in the partial saturation of the central PMT of each S2 pulse, but the long half-life will guarantee homogeneity for the purposes of calibrating the position reconstruction metrics. An additional use of this comparatively higher-energy internal source is in calibrating the xenon skin region (cf. requirement R-170008), which will possess a position-dependent detection threshold of roughly the same ~ 100 keV scale.

The hardware for $^{131\text{m}}\text{Xe}$ is nearly identical to the $^{83\text{m}}\text{Kr}$ source: xenon carrier gas is flowed over a parent isotope that is emanating the calibration isotope. In this case, the parent isotope is ^{131}I , which decays entirely to ^{131}Xe with a half-life of 8 days. A small fraction of these ^{131}I decays ($\sim 0.39\%$) are to the metastable $^{131\text{m}}\text{Xe}$ state rather than the ground state. ^{131}I is readily available from the medical isotope industry in a variety of forms. The most convenient form for our purposes is a solid pill, in which ^{131}I is doped into a solid matrix of anhydrous sodium phosphate.

The 164 keV energy of $^{131\text{m}}\text{Xe}$ decays is significantly larger than typical expected dark matter signals, and we estimate that a single PMT in the top array will experience mild analog saturation of its output signal at this energy. The saturation is a combination of exhausting the reserve charge in the coupling capacitors, and of anode saturation [1]. Nevertheless, the result of this saturation is expected to be a negligible impact on the utility of the source for (x, y, z) map-making.

7.1.3 Tritium-Labeled Methane

In addition to calibrating for position-dependent detector efficiency effects, an internal calibration source is necessary when measuring the low-energy electron recoil physics of the combined S1 and S2 energy scale, and the S2/S1 discrimination ratio (cf requirement R-170003). For this essential calibration, LUX has demonstrated the use of ^3H beta decay, exhibiting a broad energy spectrum with an 18.6 keV endpoint.

^3H decays with a 12.3-year half-life, this necessitates the ability to remove it from the xenon. This is why tritium-labeled methane is used, as it will be removed by the LZ getter (cf. requirement R-170114). LUX demonstrated that ^3H -labeled CH_4 could overcome the paired challenges of a long half life and the polymer diffusion. CH_4 exhibits a very small absorption into the PTFE, and is efficiently removed by the getter. The CH_4 purification timescale in LZ may be somewhat different from the general Xe re-circulation timescale (~ 2 d), a result of the methane's differing solubility in the liquid and gas phases of Xe. In LUX, the CH_4 purification timescale was shorter than the xenon re-circulation timescale by a significant factor, and we expect the CH_4 purification timescale in LZ to be similarly shortened.

7.1.4 Radon 220 (^{220}Rn)

^{220}Rn is being considered as a potential large-S1 calibration source for the Xe skin region. ^{220}Rn should not be mistaken for ^{222}Rn ; ^{220}Rn has no long-lived radioactive daughters, thereby making it compatible with the stringent low-background requirements of LZ. The longest-lived daughter is ^{212}Pb , with a half-life of 10.6 hours.

^{220}Rn decays through alpha decay at 6.3 MeV, followed shortly after ($t_{1/2} = 150$ ms) by a second alpha at 6.8 MeV. Alpha emission produces a highly localized and proportionally high-recombination (high-light-yield) Xe response, ideal for calibrating the skin region. Depending on the liquid mixing timescales, ^{220}Rn 's daughter isotopes (^{212}Pb , ^{212}Bi , ^{212}Po , and ^{208}Tl) are expected to accumulate on surfaces before their decay, providing a unique tool for understanding light and charge yield at xenon-surface interfaces.

Like $^{83\text{m}}\text{Kr}$ and $^{131\text{m}}\text{Xe}$, ^{220}Rn is most conveniently introduced by flowing a Xe carrier gas over a material containing the parent isotope, in this case ^{228}Th ($\tau_{1/2} = 1.9$ y). ^{228}Th can be purchased in an electroplated form, which both maximizes ^{220}Rn emanation probability and minimizes the total material (and any possible impurity content).

7.1.5 Internal Radioisotope Source Delivery

An important component of the internal calibration strategy is an effective and precise system for injecting controlled amounts of activity into the Xe circulation flow path (cf requirement R-170102). Fundamentally, the source injection system is a specialized extension of the Xe circulation system, and shares the basic design fundamentals (including the use of stainless steel VCR plumbing standards) and the basic system risks, the most important being the risk of ^{222}Rn and ^{85}Kr leakage from underground air into the circulating Xe gas. The mitigation for this radon concern is shared with the circulation system: rigorous leak testing standards during assembly, paired with enveloping the plumbing by a radon-free purge gas rather than underground air.

A schematic of the source injection system is shown in Figure 7.1.2. The source injection system will be entirely automated, both to reduce necessary onsite shift burden, and to reduce the risk to the xenon's purity from human operator error. This automation will be made possible through the general slow control system (described in Section 8.8). A connection will be in place between the source injection system and the Xe sampling system (described in Section 6.7), making it possible to perform careful checks of injection material purity before introducing any material to the flow path.

The trace amounts of radioactive gas are transported into the main circulation flow path by a small flow of Xe carrier gas, supplied by a system-specific supply of high-pressure Xe. This Xe will have gone through the same ^{85}Kr -removal process as the bulk Xe (discussed in Section 6.3), introducing no new radiopurity concerns. This small Xe flow will pass through emanation sources ($^{83\text{m}}\text{Kr}$, $^{131\text{m}}\text{Xe}$, etc.), regulated using a mass flow controller for a total mass flow roughly proportional to desired injected activity. ^3H -labeled CH_4 is injected according to a slightly different recipe; this activity is stored in a pressurized bottle, which is allowed

to fill a small evacuated ‘dosing region’ volume to a precisely-measured pressure. This dose volume will then be flushed by the Xe carrier gas into circulation, as with the flow-through sources. The internal source injection system is being designed to be general and flexible, allowing for alternative injection procedures and for the possible use of internal sources not yet developed.

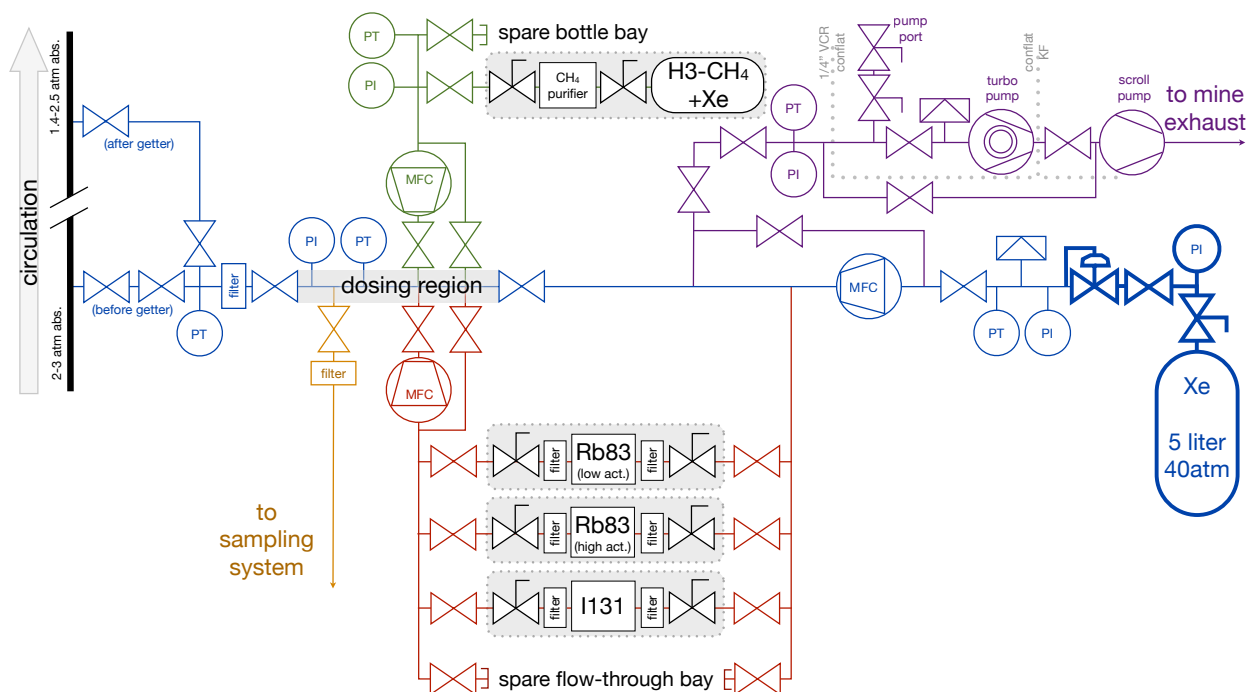


Figure 7.1.2: The internal radioisotope source delivery system is a portion of Xe plumbing with the goal of releasing a precise portion of various gaseous radioactive isotopes into the main xenon circulation path. This control is achieved through a combination of Mass Flow Controllers (MFCs) and Pressure Transducers (PTs), with flow from the dosing region into the circulation path (far left) motivated by a high-pressure Xe supply bottle (far right).

7.2 External Radioisotope Source Delivery

LZ will have three stainless steel vertical source tubes in the vacuum space between the inner and outer titanium cryostats, as shown in Figure 5.3.1. The calibration source deployment (CSD) system will position neutron and gamma calibration sources in the source tubes. The source tubes will have an inner diameter of 23.6 mm, large enough to accommodate deployment of commercial sources in nearly all cases. The necessary source strengths are well within the available range. Sources that cannot be obtained commercially in our requisite dimensions and rate will be fabricated by LZ (University of Alabama). The source tubes will be sealed at both ends and kept in a nitrogen atmosphere at a pressure of 1.1 bar to suppress contaminants entering the system and prevent the plating of radon daughters. The photoneutron and DD neutron sources require dedicated deployments and are discussed separately below.

7.2.1 Neutron sources

A suite of four neutron sources will provide a broad-spectrum NR calibration, with the additional benefit of four distinct kinematic endpoints, as shown in Figure 7.2.1. In particular, these broadband sources are useful for measuring the NR band (cf. requirement R-170004). Also shown in the figure are the nuclear recoil detection efficiencies for 2- and 3-fold PMT coincidences. 3-fold coincidence is the baseline for WIMP search analysis, but in calibrations, where the total data taking time is much shorter, 2-fold PMT coincidence thresholds may be more appropriate for understanding low-energy response of the detector.

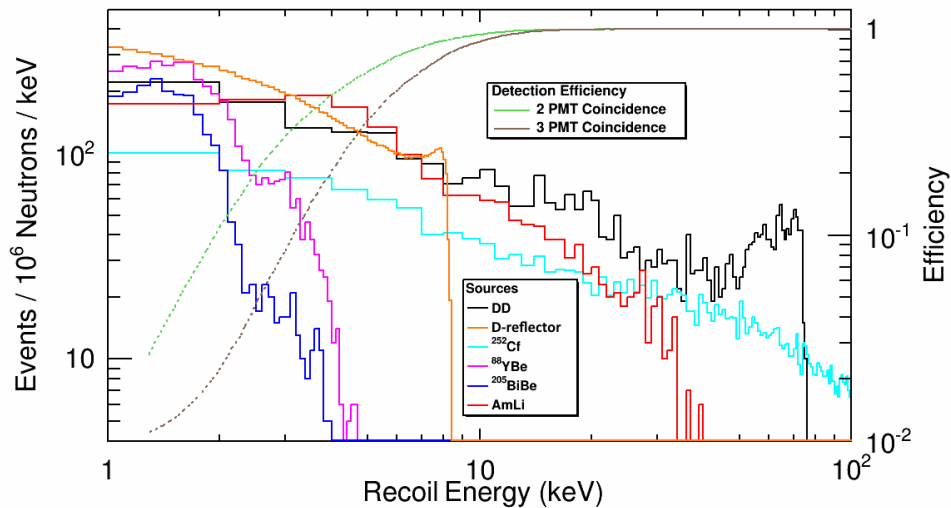


Figure 7.2.1: Recoil spectra obtained from each of the primary neutron sources, DD (black), DD back-scatter off deuterium (orange), ^{252}Cf (cyan), YBe (red), BiBe (blue), and AmLi (magenta). 1 million neutrons corresponds to roughly three hours of calibration with a 100 neutron/s source. The scalings for DD and DD deuterium back-scatter ("D-reflector" above) are arbitrary. These calibrations can easily achieve the single-scatter statistics required and their main goal is to use the double-scatter events. Shown on the y-axis on the right is the nuclear recoil detection efficiency for 2 and 3 fold PMT coincidences.

AmBe (α, n) neutron sources have typically been the broad-spectrum neutron source of choice, as they cover the range from threshold to in excess of 300 keV recoil energy. The motivation to also use an AmLi source is the lower maximum neutron energy of about 1.5 MeV, which results in a fairly distinct endpoint at about 40 keV. Simulations show that the yield of single-scatter NR candidates with energy less than 25 keV is comparable to AmBe but with an enhanced fraction of events at low recoil energy (less than 10 keV). The rates shown in Figure 7.2.1 would be obtained in about three hours of live time, assuming 100 neutron/s source strength. It is notable that the (α, n) yield is lower for AmLi than for AmBe, so that a higher americium activity of about 2.5 mCi is required to obtain a source strength of 100 neutron/s. The sources will be encapsulated and there are no additional safety concerns.

A generic result of the (α, n) reaction is that the product nucleus may be in an excited state, leading to the release of a gamma. With AmBe, the most common gamma energy is 4.4 MeV and it occurs in 58% of decays. No literature exists for this process with AmLi sources. Our own preliminary measurements indicate that final state gammas occur at the percent level.

7.2.2 Gamma Sources for Calibration of the Active Xe TPC

External gamma sources are not required for any of the primary calibrations of the active Xe TPC. This is by design, as the active region is self-shielded against external gammas. Nevertheless, several important calibrations will be obtained from external gammas. These include studies of higher-energy backgrounds and signal fidelity near the edge of the TPC. A single ^{228}Th (2,615 keV) source serves this purpose and, in addition, helps provide a calibration of the outer detector.

7.2.3 Gamma Sources for Calibration of Xenon Skin and the Scintillator Veto

The detection thresholds for the Xe skin veto and the organic scintillator veto are 100 keV and 200 keV respectively. Various sources (cf. Table 7.0.1) will be deployed in the source tubes to verify this performance (cf. requirement R-170008 and R-170009). Calibration of the outer detector energy scale (cf. requirement R-170009) is achieved with a ^{228}Th source as shown in Figure 7.2.2. The simulated response as a function of Z in the Xe skin is also shown in Figure 7.2.2. For the timing synchronicity calibration between the outer detector and the skin, a ^{22}Na source will be deployed (cf. requirement R-170010). The source produces simultaneous back-to-back 511 keV gammas which can be observed in the outer detector and the TPC to look for any difference in timing.

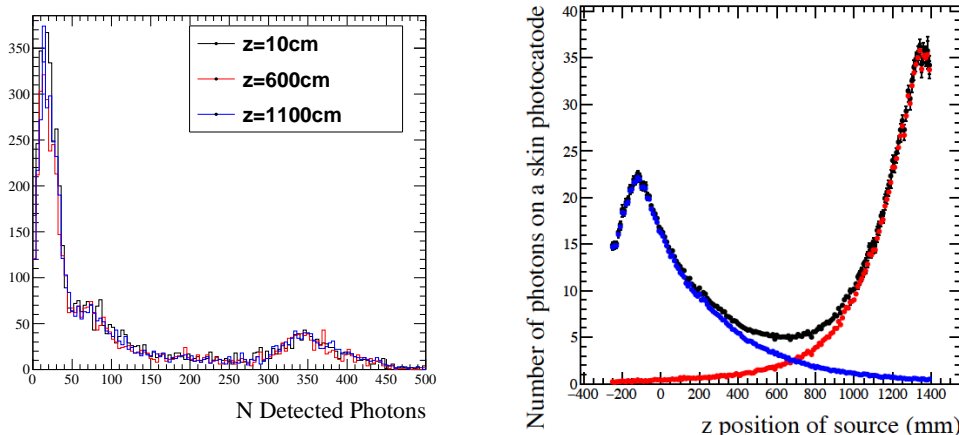


Figure 7.2.2: Number of measured photons detected versus Z-position in the outer detector (left panel, ^{228}Th source) and the xenon skin (right panel, ^{57}Co source). The ability to study the performance of the Xe skin as a function of the Z-coordinate motivates the need to be able to locate a source to within 5 mm (cf. requirement R-170201)

7.2.4 Calibration Source Deployment (CSD)

Figure 7.2.3 shows the design of a prototype assembly developed to define the core design and components of the CSD. The source deployment system consists of a stepper motor (a SANMOTION F2 2-phase stepping motor model SH2141-5511 with a resolution of 1.8° manufactured by SANYO DENKI Co) coupled to the planetary gear-head GP 22A with a 19:1 reduction (manufactured by Maxon). The gear unit couples the stepper motor to a drum holding the deployment filament and source. The deployment filament is a strong thin nylon composite (~ 0.1 mm diameter, maximum load 12 kg) that carries the load of the source assemblies

(~100 g) with a 4× safety factor. The CSD covers the full 6 m length of the upper and lower calibration tube from the top of the water tank to beyond the cathode level. The CSD mechanics is housed in a K50 Tee-piece that couples via a connection chamber sideways to the calibration source tube making it a very compact system. The stepper motor and gear are held in a support structure clamped to the T-piece. A wheel on a lever feeds the filament from the drum into the calibration tube. Each calibration tube will be fitted with its individual deployment system; the three systems are configured to enable simultaneous operations. A prototype using the same design has been tested at RAL to ensure that thousands of source deployments are possible without failure (cf. requirement R-170202).

As additional control on the z-position of the calibration sources, each deployment system will be fitted with a laser based position monitoring system. For this an ILR1181-30 Micro-Epsilon laser ranger will be coupled to the top of the connection chamber allowing an accurate (better than 2mm precision) reading of the source position. The monitoring system will be incorporated in a feedback protocol that drives the CSD system and thus ensures the z-position accuracy of ± 5 mm is met (cf requirement R-170201).

Each system is driven by a ZYBO FPGA board and a PMODSTEP daughter board both manufactured by Digilent. This system allows computer control of the deployment, provides feedback of the operational parameters and will be fully integrated in the Run Control structure.

An unacceptable failure mode of this system would be a source detached from the deployment filament dropped to the bottom of the tube. As a control against this eventuality, the sources are fitted with a ferromagnetic component which allows retrieving sources with a magnet. A full scale mock-up of the design of this system is constructed and extensively tested.

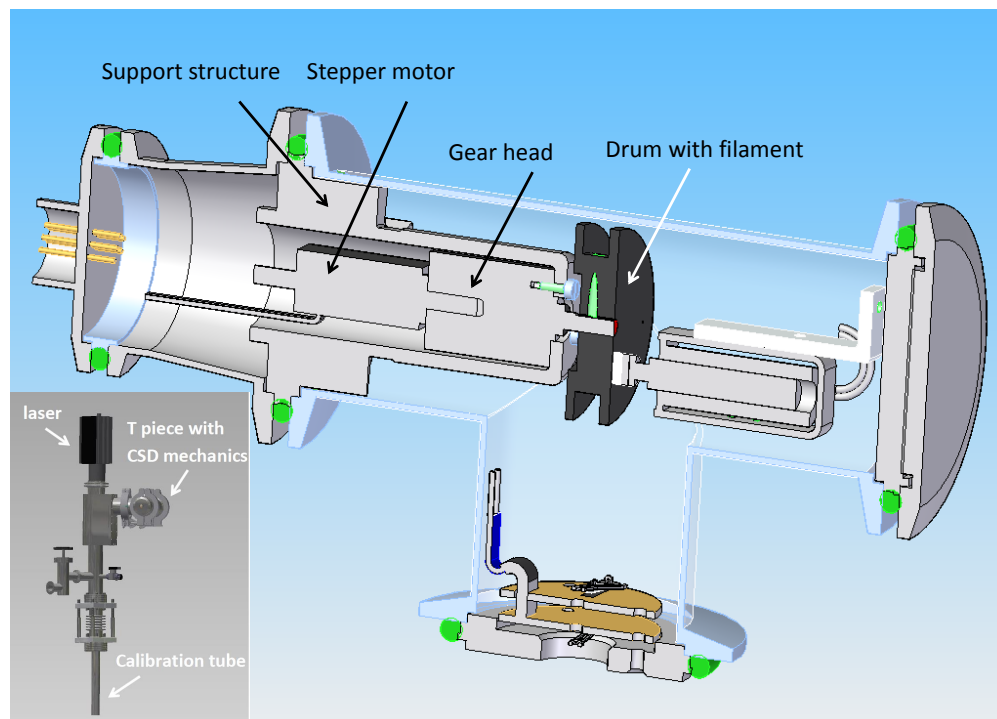


Figure 7.2.3: The prototype assembly developed to define the core design of the CSD system: the stepper motor and gear are held in a support structure clamped to the T-piece. The T-piece couples sideways via a connection chamber to the calibration tube as shown in the inset.

7.2.5 Radioisotope Capsule Design

Most sources for use in the CSD will be commercial Eckert & Ziegler (E&Z) type R sources. The source form factor is a 5" long X 0.625" diameter acrylic cylinders with the source epoxied and encapsulated at one end. The bare acrylic end of the cylinder (the end without the source) will be tapped with an M4 hole, in order to connect to the CSD. The monofilament is captured in a vented screw, which itself secures a martensitic stainless steel (410SS) ring collar to the top of the acrylic cylinder. The use of this ring allows a simple, robust magnetic recovery system can be deployed in the unlikely event of a break in the monofilament which suspends the source.

The AmLi source will be custom fabricated at the University of Alabama since commercial versions are not available in our requisite form factor. Custom sources will have the same form factor and mating structure as commercial sources. Preliminary activities of these sources have been determined. Simulation effort to validate the choices are on-going (cf. requirement R-170301).



Figure 7.2.4: Prototype dummy source capsule showing 410SS ring with magnetic recovery system attached.

7.3 Photoneutron Sources

As discussed in Section 2.2.1.2, coherent scatters from ^8B neutrinos pose a potential background in LZ as they are difficult to distinguish from a light mass WIMP. However, higher WIMP masses are unaffected by this issue assuming the signal from such recoils is well understood. Having a calibration targeted at understanding the response of LZ to these low-energy scatters is critical. Because of their well-defined kinematic endpoint, photoneutron sources are the most important tool for this purpose and help to fulfill requirement R-170005.

7.3.1 Physics of Photoneutron Sources

Photoneutron sources exploit (γ, n) reactions on nuclei to produce neutrons. Suppose there is an incident gamma of energy E_γ incident on a nucleus. That nucleus has some threshold, Q , for emission of a neutron by (γ, n) . If $E_\gamma > Q$ there is some finite probability for the nucleus to absorb the gamma and emit a neutron with energy [2]

$$E_n(\theta) = \frac{M(E_\gamma - Q)}{m + M} + E_\gamma \cos(\theta) \sqrt{\frac{(2mM)(E_\gamma - Q)}{(m + M)^3}} \quad (7.3.1)$$

where M is the mass of the nucleus and m is the mass of the neutron. The second term, which has an angular dependence, as θ is defined as the emission angle of the photoneutron relative to the direction of the incident gamma ray. The angular dependence causes a relative difference of 4.6 % in the emitted neutron energy between $\theta = 0^\circ$ and $\theta = 180^\circ$ for $^{88}\text{Y Be}$ source (described below). This energy difference is similar to the end point energy difference caused by isotopic spread (5 % between ^{129}Xe and ^{136}Xe). Thus, photoneutron sources can be considered to produce mono-energetic neutrons. One example of a photoneutron source used by [3] was a $^{88}\text{Y Be}$ source, with $E_\gamma = 1.836 \text{ MeV}$ and $Q = 1.666 \text{ MeV}$, producing 153 keV neutrons. A technical challenge of deploying a photoneutron source is that the cross sections for (γ, n) are generally very low. For example, in [3], a 1.85 MBq ^{88}Y source was used and ~ 330 neutrons/second were generated. That

is $>5,000$ gammas per neutron. For practical purposes such sources need a large amount of lead or tungsten shielding to reduce the gamma rate in the detector, while preserving a useful neutron flux.

Two sources of interest for LZ are ^{88}Y Be and ^{205}Bi Be. ^{205}Bi Be creates neutrons of three different energies, the dominant one having an energy of 88.5 keV, with a nuclear recoil end point of $2.7\text{ keV}_{\text{nr}}$ in Xe. The nuclear recoil end point from a 152 keV neutron from ^{88}Y Be is $4.6\text{ keV}_{\text{nr}}$. Figure 7.3.1 shows a comparison of the signals in LZ from ^8B to the photoneutron sources. ^{88}Y Be bounds the end point for the ^8B spectrum while ^{205}Bi Be is more similar to the spectrum which would be observed from a 1,000-day exposure. Note that because the source is above the detector, most of the neutron scatters occur near the gate and have short drift times. Although the calibrations will contain a large number of gamma interactions, they are easily separated from the nuclear recoils by their apparent energy. The ER events are dominated by neutron capture gammas, as there is enough tungsten shielding in the design to make the gammas directly from the ^{88}Y or ^{205}Bi decay negligible.

7.3.2 Photoneutron Source Deployment

Photoneutron sources will be deployed in a 20 cm diameter \times 20 cm tall cylindrical tungsten alloy pig from above LZ. The pig will weigh 116 kg and the cryostat is rated to hold this weight (cf. requirement R-170401). During calibrations the pig will sit on top of the outer cryostat vessel, on axis. Figure 7.3.2 shows the individual components and the overall deployment scheme. The pig will be lowered through a stainless steel guide tube from three points. The guide tube has a funnel top to accept the pig and holes in the side to

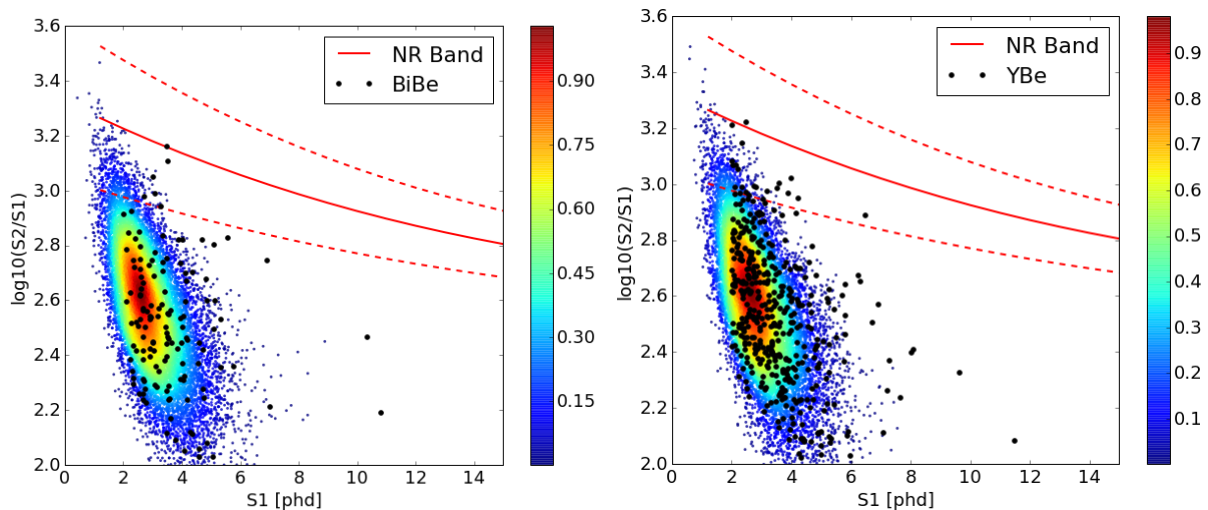


Figure 7.3.1: Comparison of S1 versus S2 spectra for ^8B solar neutrino coherent scatters versus ^{205}Bi Be (top) and ^{88}Y Be (bottom) in LZ. The ^8B spectrum is a two dimensional PDF represented by the arbitrary color scale. The black dots are the neutron events and the red curves are the nuclear recoil band. The neutron events come from simulation. Events that appear to be at higher energy are the result of multiple scatters, some of which would pass all cuts in a real analysis. Here a 2-fold PMT coincidence cut is assumed, as the live time of these calibrations will be short compared to WIMP search and all the real events will have short drift times. This results in a very low rate of accidental S1+S2 coincidences. The above plot corresponds to 30 hours of calibration with a 100 neutron / s, indicating that with a reasonable activity source, one can perform this calibrations in a few days (cf. requirement R-170404)

displace water. There must be minimal water trapped underneath the tungsten (cf. requirement R-170402) and this is achieved by keeping the relevant surfaces relatively flat. There are two critical safety measures designed into this process to protect the cryostat and the experiment. First, the water above the cryostat acts as a cushion, slowing the descent of the pig. Second, the three lifting points are redundant, so even if one cable breaks, the other two can support the weight of the pig. In the unlikely event that the pig were to get stuck in the guide tube, the source is separately removable. Furthermore, the entire guide tube can be removed with the pig in it.

7.4 Deuterium-Deuterium Neutron Source

A deuterium-deuterium (DD) neutron source, the Adelphi Technologies DD109 neutron generator, will be deployed in the LZ experiment for nuclear recoil calibrations. The generator that will be set up outside of the LZ water tank can produce up to 10^9 mono-energetic 2.45 MeV neutrons per second into 4π . Conduits in place within the LZ water tank provide a path for neutrons to travel through the water tank and outer detector to reach the Xe volume within the detector (Figure 7.4.1). So as not to degrade the energy of the neutrons, the amount of water in their path needs to be kept small (cf. requirement R-170501). This novel in-situ NR calibration technique has been successfully implemented in the LUX experiment to calibrate the absolute energy response of NR in LXe down to $1.1 \text{ keV}_{\text{nr}}$ for light yield (Ly) and $0.7 \text{ keV}_{\text{nr}}$ for charge yield (Qy) with significant improvements to the calibration uncertainty[4] and has helped improve the LUX detector sensitivity to low-mass WIMPs by orders of magnitude[5].

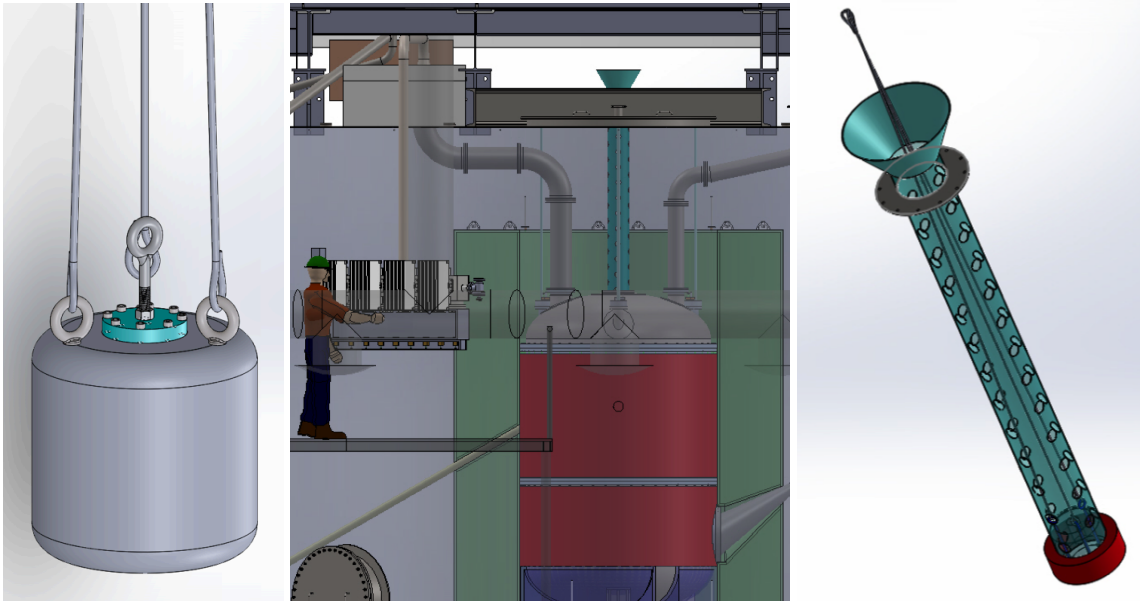


Figure 7.3.2: From left to right: Photoneutron pig (20 cm outer diameter \times 20 cm height tungsten) suspended from three points, side view of the guide tube in-place on top of the cryostat, guide tube (8.25 inch outer diameter \times 8.0 inch inner diameter stainless steel) on its own with the funnel top to accept the pig.

7.4.1 Physics motivation of Deuterium-Deuterium Neutron Sources

This technique will be further upgraded in LZ to explore even lower energy NR response to reduce calibration uncertainty. Four types of measurements are planned to be carried out in LZ using the D-D neutron source as described in the following subsections.

7.4.1.1 NR Qy / Ly calibration of the LZ detector

In the DD calibrations implemented in LUX, double-scatter events in LXe due to mono-energetic 2.45 MeV neutrons are used to calibrate the NR charge yield (S2) response[4]. The absolute deposited energy in the first scatter can be determined by measuring the neutron scattering angle between it and a second scatter. Given the deposited energy, the Qy can be determined by estimating the number of electrons produced at the first scatter. The light yield (S1) can then be inferred by using the calibrated S2 signal to assign an energy deposited to single-scatter events[4]. This calibration technique using 2.45 MeV neutrons covers WIMP search energy range (requirement R-170010) from threshold (6 keV) up to 30 keV (Figure 7.2.1) with an additional endpoint at 74 keV.

7.4.1.2 Calibrating LZ detector using Reflected Neutrons from D2(O) Target

As discussed in Section 7.3, an understanding of the LZ response to recoil energies at the threshold (requirement R-170005) is critical to probe low mass WIMP and ^8B solar neutrino signals. By placing a deuterium-loaded reflector behind the DD generator and collecting the neutrons that are reflected at a near-180 degree angle (Figure 7.4.1), the generator's direct 2.45 MeV neutron flux can be converted into a quasi-mono-energetic neutron beam with a minimum energy of 272 keV. These lower energy neutrons can be used to calibrate in a new energy regime. Lower energy neutrons provide smaller uncertainty, because the angles are more favorable. In addition, the recoil spectrum endpoint in Xe is reduced from $74 \text{ keV}_{\text{nr}}$ to $8.2 \text{ keV}_{\text{nr}}$, thus confining the neutron scatters to within this lower energy region of interest (1 to 8 keV). In addition, the slower incident neutron speed would provide greater separation in S1 times for double scatters, which would assist in the direct Ly calibrations planned for LZ (Section 7.4.1.4).

7.4.1.3 Calibrating LZ Detector with Neutron Events with no S1 Light

Another technique to calibrate LZ response at threshold (requirement R-170005) is to explore neutron events with no scintillation light. This requires an additional tool to establish t_0 for the electron drift of a neutron event, which is usually determined by S1. This additional tool is given by shorter neutron production pulses, resulting in tighter bunches of neutrons. In LZ, our plan is to upgrade the Adelphi Neutron Generator such that it is capable of reducing the neutron bunch width down to the few-microsecond level (as shown in Figure 7.4.2). The neutron trigger pulse will be digitized by one of the DAQ channels to synchronize with other channels that digitize PMT signals. This allows identification of t_0 . There are two direct benefits of implementing this technique. First, it provides an additional timing cut that helps significantly to reduce neutron analysis background events. Second, it allows probing no-S1 neutron events; the measured number of DD scatters with a known number of zero-collected-photon S1 pulses provides considerable statistical leverage and provides a stronger constraint on Ly because the number of no-S1 events can serve as a normalization for the observed number of $S1 > 0$ events.

7.4.1.4 Direct Ly Measurement Using Double (Multiple) Scatter Events

A direct light yield measurement will significantly reduce the systematics in the existing technique (Section 7.4.1.1). A direct light yield measurement in LUX is not feasible because S1 light from two scatters

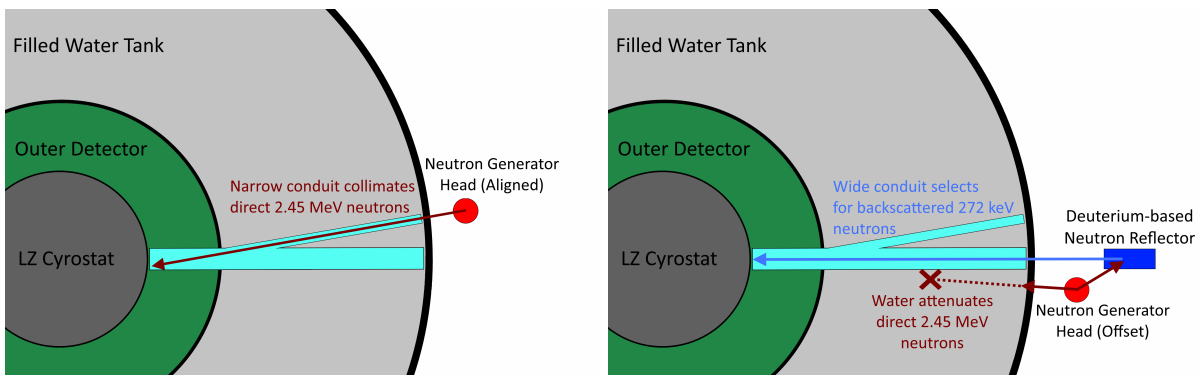


Figure 7.4.1: Approximate setup of the DD generator and neutron conduits. The y-shaped conjoined tube allows for a choice between finer collimation with lower flux by using the smaller, 5.25 cm inner diameter tube and broader collimation but greater flux by using the larger 15.4 cm inner diameter tube. The smaller tube joins the larger one in a bonded joint just outside the outer detector, though the path of the neutrons from the smaller tube continues up to the cryostat wall. (Left) The configuration for 2.45 MeV calibration. The neutrons go directly from the generator to the detector through the narrow conduit. (Right) The configuration for 272 keV calibration. The generator head (red) is offset from the neutron conduit to prevent direct neutron flux into the xenon via water attenuation by the water tank, while neutrons reflected off the deuterium reflector (blue) may enter via the air-filled neutron conduit (cyan).

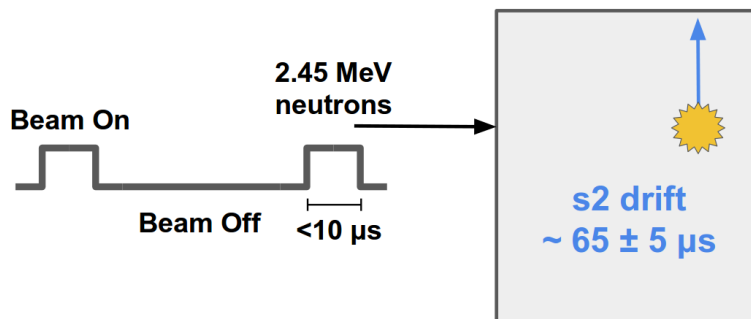


Figure 7.4.2: The square wave on the left indicates the DD trigger pulse. The schematic on the right indicates a no-S1 single-scatter neutron event based on a tube centered 12.5 cm from the LXe surface. The z position resolution from the DD trigger is comparable to the x, y position of such events. As described in the text, this technique gives additional capability to probe nuclear recoil response at threshold.

overlaps in time. However, given that the LZ LXe volume is at the meter scale, it is possible to separate S1 signals from the first two scatters in a double (multiple) scatter D-D neutron event by leveraging the time of flight of neutrons in greater path lengths in the LZ LXe volume, especially for 272 keV neutrons, whose speed is a factor of 3 lower than 2.45 MeV neutrons but have similar scattering cross sections, and thus take significantly longer for the second scatter to occur on average Figure 7.4.3. This will thus allow a direct light yield measurement by using double (multiple) scatter events in a similar way to measuring Q_y in the standard calibration, helping eliminate the systematics due to S2-energy mapping in the indirect L_y measurement.

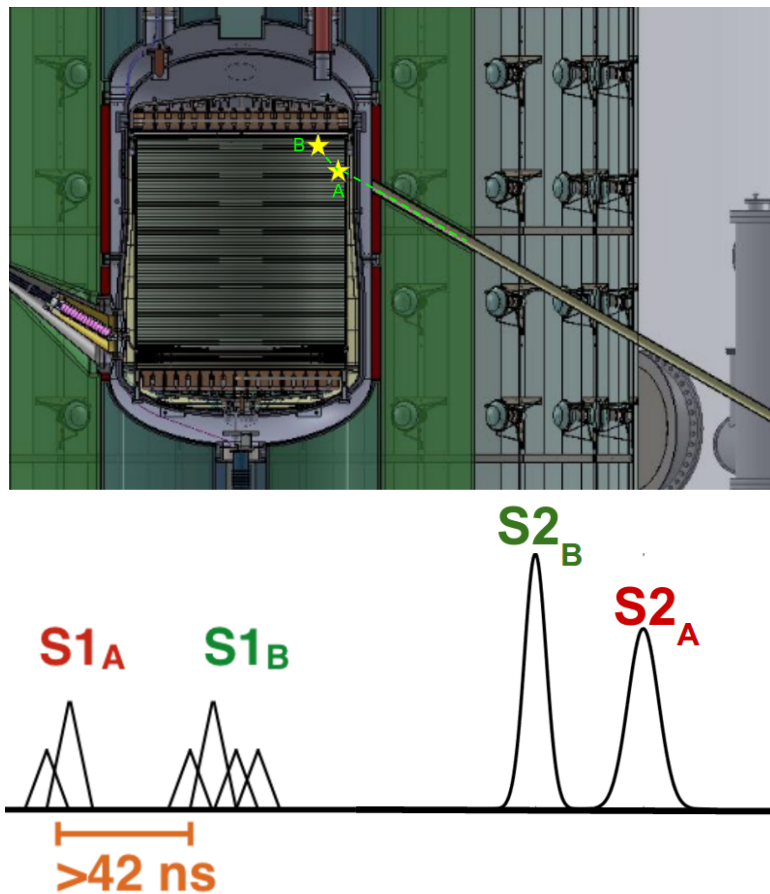


Figure 7.4.3: Top shows the solid model of LZ detector with angled neutron tube. The leveled tube is not shown in this figure. A cartoon neutron double scatter event in the scenario of separated S1s is also shown in the figure. Bottom shows the expected waveform of a neutron double scatter event with two separated S1s.

7.4.2 DD Source Deployment and Neutron Rates

The generator, manufactured by Adelphi Technology Inc, uses deuterium-deuterium (DD) fusion to generate neutrons at 2.45 MeV. D₂ gas is pumped into a chamber where it is ionized via RF induction discharge. A titanium plate is biased using a negative high voltage between -80 and -125 kV, which draws the D⁺ ions. The ions embed in the titanium plate, forming titanium hydrate. Subsequent ions strike the embedded ions and eject neutrons via the fusion reaction $D+D \rightarrow {}^3\text{He}+n$. At maximum operating parameters, the generator is designed to output 10^9 n/s into 4π . [6]

The DD generator is located outside the LZ water tank. The neutrons will be collimated via two sets of tubes inside the water tank, each of which has two options for the diameter: a 16.8 cm outer diameter tube and a 6.03 cm outer diameter tube. (See Figure 7.4.1 for a drawing of the two-diameter approach and Figure 7.4.3 for a depiction of the angled tube.) During WIMP search, the tubes are filled with water, thus maintaining the water shielding around the detector. During calibrations, the tubes are drained of water and filled with a nitrogen purge, which allows the neutrons to pass into the detector. One tube is horizontal and will be centered 12.5 cm below the LXe surface, while one is angled 20 degrees to the horizontal, the

center of which enters the LXe volume 40.5 cm below the LXe surface. The horizontal tube mimics the implementation of the LUX DD tube, which has been used to great effect, while the angled tube seeks to take advantage of the preferential forward scattering via the higher precision in z -coordinate reconstruction.

The generator itself will be mounted on a platform supported by a modified SLA-10 (Super Lift Advantage) Genie lift. This lift can be moved to either neutron conduit site and will be capable of raising the generator head to the entrance of both neutron conduits. Form-fitting generator shielding will adequately reduce neutron flux in the Davis Cavern, and plugs in the shielding at both conduit angles will be added or removed to allow for maximum flux into the desired conduit.

For the DD backscatter calibrations, the generator head is placed off-axis of the neutron conduit while a backscatter target is aligned with the conduit. As the neutrons are produced by the generator head, those hitting the deuterium backscatter target scatter at a near 180° angle and are sent down the conduit to the interior of LZ, while direct neutron flux is attenuated by the water tank. Kinematically, the 180° backscatter results in a reduction in neutron energy from 2.45 MeV to 272 keV. Losses in neutron flux due to backscattering will be compensated by a heightened generator neutron flux (up from 4×10^6 n/s to 1×10^9). The diameter of the neutron conduit (15.4 cm ID) is driven by the need to get enough flux in deuterium backscatter calibration.

7.5 Calibration Rates

In general, event rates in the LZ detector of course depend on source location, type and energy spectrum. For neutron calibrations, a number of generally applicable conclusions can be obtained from the representative case of 2.45 MeV neutrons emanating from the wall of the outer Ti cryostat vessel. The scenario is identical to what would be realized during a DD neutron calibration, assuming neutrons that strayed out of the conduit do not contribute appreciably to the event rate in the Xe TPC. The scenario is also qualitatively similar to the foreseen AmLi calibration, obtained from a source located in one of the three external source tubes.

7.5.1 Effect of Gd doping in liquid scintillator

A generic concern for neutron calibrations of the Xe TPC is that Gd doping of the liquid scintillator in the outer detector will cause a large rate of gamma events in the Xe TPC. Monte carlo simulations suggest that this concern is not warranted. As shown in Figure 7.5.1, the event rate due to neutron captures on Gd is only slightly larger than it would have been with undoped liquid scintillator, and only in the energy window $2.2 \text{ MeV} \lesssim E \lesssim 4.0 \text{ MeV}$.

7.5.2 Effect of gamma captures on useful neutron event rates

A key number for neutron calibrations is the fraction of useful events. As mentioned above, this will depend on the geometry and energy of the source. Table 7.5.1 provides numbers for the simplified, representative case described at the beginning of Section 7.5. Shown are fractions of neutrons events for various scenarios. Single scatters with gamma veto provide the relevant useful event fractions for defining the NR band. $\sim 3\%$ of neutrons result in a useful single-scatter in the detector, after removing events that contain any ER component. Double scatters with gamma veto provide the relevant useful event fractions for most DD studies.

7.5.3 Maximum useful calibration rates

The maximum useful calibration rate will in most cases be driven by the drift time of the TPC. This limitation can be circumvented by delivering events near the top of the TPC, in order to shorten the drift time. However,

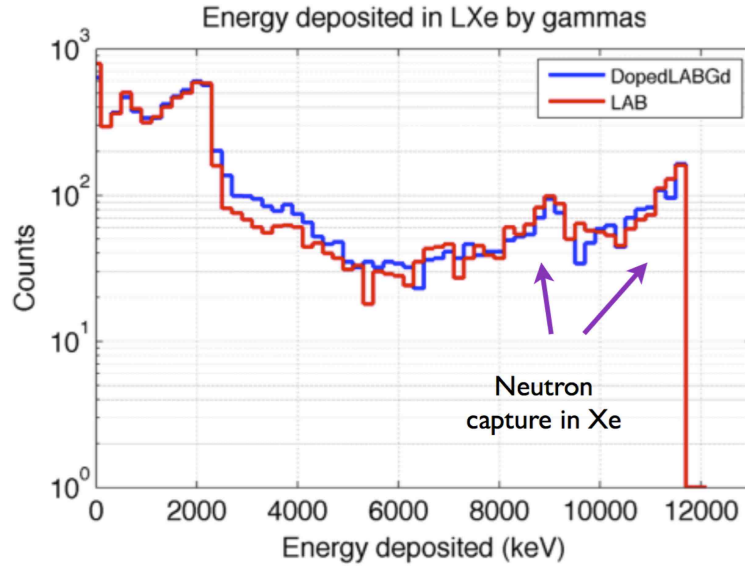


Figure 7.5.1: Event rate due to gammas in the xenon TPC from neutron captures on Gd.

Table 7.5.1: Fraction of neutron scatters in the Xe TPC for various assumptions about the outer detector material in the acrylic vessels. Gd doped LAB is the baseline choice. LUX, which has only H₂O outside the TPC, is shown for reference. Also shown for comparison to make the impact of LAB and Gd doping clear are LZ with LAB only (no Gd doping) and water instead of scintillator.

	LZ			LUX
	Gd-doped LAB	LAB	H ₂ O	-
single scatters (no cuts)	0.129	0.123	0.115	0.266
single scatters (γ veto)	0.032	0.031	0.033	0.164
double scatters (no cuts)	0.106	0.107	0.114	0.073
double scatters (γ veto)	0.020	0.025	0.026	0.042

in the interest of understanding the most general case first, the projections shown in Figure 7.5.2 assume an event window defined by twice the maximum drift time.

For an average event rate λ in a time window t_w , the probability to obtain n or more random events in any particular window is given by

$$P = e^{-\lambda} \sum_{n=1}^{\infty} \frac{\lambda^n}{n!}, \quad (7.5.1)$$

from which Figure 7.5.2 is derived. A 10% pileup rate could be achieved by keeping the calibration rate below 50 to 70 Hz, depending on the drift time.

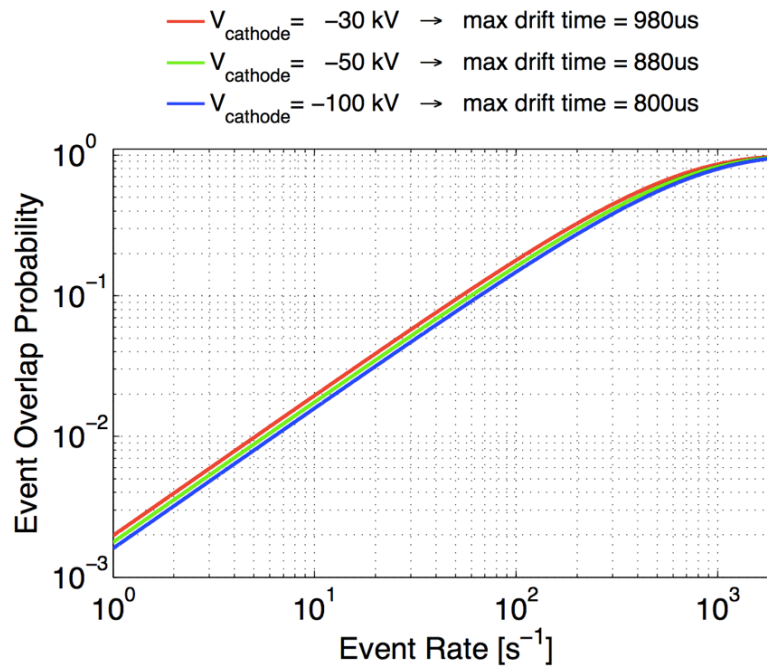


Figure 7.5.2: The electron drift time produces a time window in which an unrelated event could produce S1-S2 pairing confusion. The Poisson probability of event overlap is plotted here, and provides an estimate as to the maximum calibration rate in LZ for a desired maximum event overlap probability, for a specified field configuration (electron drift velocity), and a specified event distribution in z . Here, we assume all calibration events are at the position of longest drift time, and vary the field configuration according to several possible running modes. If a 10% overlap probability is acceptable, then the bottom of the detector could be calibrated at 50 to 70 Hz.

7.6 Environment, Health and Safety Concerns

Safety concerns related to calibrations mainly relate to the use of radioactive sources. Most sources are either internal, and therefore don't expose users to radioactivity, or are NRC exempt. The most active source to be used in LZ is the DD generator, which will be capable of producing 10^9 neutrons/second. This source was also used in LUX and the safety concerns were mitigated by having an exclusion zone around the generator while it is operating. Because the generator can be operated remotely, no one needs to be inside this exclusion zone during operation. For LZ there is a planned 9 m exclusion zone. Points inside and outside this exclusion zone will be monitored with neutron detectors to ensure the areas where work will continue to take place are still safe.

Photoneutron calibrations require gamma sources with activities up to 3 MBq (81 μCi) which are not NRC-exempt. However because these sources will always be deployed inside of a tungsten shield, there is no reason they can't generally live inside an insert with a small amount of shielding to protect the users. Only briefly upon initial receipt of a source does a user need to handle one outside of such shielding. Specific safe handling procedures are under development.

7.7 Bibliography

- [1] Hamamatsu Photonics K. K., *Photomultiplier Tubes: Basics and Applications* (2007), Third Edition (Edition 3a).
- [2] G. F. Knoll, *Radiation Detection and Measurement* (John Wiley & Sons, Hoboken, NJ, USA, 1989).
- [3] J. I. Collar, *Phys. Rev. Lett.* **110**, 211101 (2013), arXiv:1303.2686 [physics.ins-det].
- [4] D. S. Akerib *et al.* (LUX), “Low-energy (0.7-74 keV) nuclear recoil calibration of the LUX dark matter experiment using D-D neutron scattering kinematics,” (2016), submitted to *Phys. Rev. C*, arXiv:1608.05381 [physics.ins-det].
- [5] D. S. Akerib *et al.* (LUX), *Phys. Rev. Lett.* **116**, 161301 (2016), arXiv:1512.03506 [astro-ph].
- [6] *DD-108M Neutron Generator Operation Manual*, Adelphi Technologies Inc., 2003 E. Bayshore Rd., Redwood City, CA 94603 (2012).